International Journal of Enhanced Research in Management & Computer Applications,
ISSN: 2319-7471, Volume 14 Issue 7, July 2025

AI Detection through Numeric Logic and Geometric Visualization: Scaffolding Complex Structures for Multidisciplinary Critical Analysis

Farida Bouattoura

Doctoral Candidate

ABSTRACT

Detecting artificially engineered informational biases requires methods that transcend traditional analytical approaches. Conventional detection tools often overlook complex numeric structures intentionally embedded within textual narratives. Addressing this gap, the current research provides a structured numeric logic approach enhanced by geometric visualization, explicitly designed to scaffold complex mathematical relationships into intuitively understandable frameworks. By beginning with fundamental numeric concepts, such as simple points and linear equations, the analysis systematically builds toward the detection of sophisticated, algorithmically generated textual biases. Central to this method is the Farid–El Djezairi triangular structure, which visualizes numeric ratio data across various analytic layers, yielding clear geometric patterns (hexagonal, hexagram, pentagonal, and pentagram). The adaptability of this numeric-geometric method is further demonstrated using standard computational tools such as Google Sheets, providing democratic access that makes sophisticated AI detection techniques available to a diverse, multidisciplinary scholarly audience. Numeric logic is intentionally structured and scaffolded to reveal engineered directionalities through explicit geometric transformations, clearly revealing intentional numeric biases hidden within complex texts, particularly those relating to human rights reporting and geopolitical strategies. By democratizing complex mathematical and technological concepts, the research empowers analysts and scholars across various disciplines to critically and effectively engage with AI-generated narratives and algorithmic disinformation. The deliberate simplicity and accessibility of this fibristic epistemological approach represent a significant advancement in AI detection and critical literacy, enabling broader participation in evaluating discourse influenced by algorithms.

Keywords: AI Detection, Numeric Logic, Geometric Visualization, Critical Literacy, Algorithmic Bias, Fibristic Epistemology, Structured Numeric Analysis, Democratic Access, Scaffolded Mathematics, Multidisciplinary Analysis.

INTRODUCTION

The inception and approach of the method began from the most fundamental mathematical concepts, such as defining numeric positions starting simply from a point and progressively building into more complex, systematic relationships. The purpose was to remove the technical and mathematical jargon that typically acts as a gatekeeper for individuals in liberal arts or related fields, preventing them from accessing or understanding content traditionally dominated by complex notation or calculus. Instead, the method presented herein was intentionally crafted to ensure internal coherence and intuitive logic, enabling all readers to understand the detailed weaving of numeric structures and relationships. Such an accessible approach scaffolds knowledge for readers, intuitively demonstrating practical applications. The practical application presented here shows the indispensable utility of fibristic analysis in critical fields, including human rights reporting, geopolitical strategy, and institutional risk mitigation. By emphasizing numeric clarity and procedural precision, fibristic epistemology empowers analysts to identify embedded logical structures, engineered biases, and implicit directionalities—nuances that conventional AI tools or traditional detection methodologies would likely overlook (Bouattoura, 2025c). Such a structured, rigorous approach is essential for addressing contemporary informational challenges, enhancing critical literacy, and enabling stakeholders to maintain objectivity and integrity amidst increasingly sophisticated and covert algorithmic disinformation campaigns. Moreover, this scaffolding highlights the deterministic nature inherent in algorithmic logic and computer coding, illuminating readers about implicit and covert disinformation or propaganda campaigns. Critical literacy here reveals that misinformation or disinformation can follow multiple pathways and directions, including deliberately weighted logical distributions. Therefore, readers must analyze information objectively and critically, ensuring they do not unintentionally promote or reinforce a constructed narrative. Such a structured numeric design does not require outright false information; rather, it strategically instruments arguments and premises to fit predetermined logical patterns. Consequently, expertise in critical literacy, logic, and law, paired with objectivity, becomes essential for accurately recognizing and evaluating systematically engineered informational constructs. The guiding question for this research is:

How can numeric logic and directional analysis, informed by fibristic epistemology, illuminate systemic biases and engineered structures within complex informational constructs?

Fundamental Numeric Framework and Directional Pathways

To commence our research in an accessible manner, we begin with the simplest mathematical element—a point. Limiting our units to either 1, 0 (representing no unit), or -1 (in a bidirectional sense) provides a conceptual link. The most straightforward practical analogy for this numeric concept, especially if it feels intangible, can be imagined in terms of money—one can have one unit, have no units, or owe a unit. Consider starting with the initial triadic numbers 1, 0, and -1, defined within a numeric range from -1 to 1. Beginning from the initial point of zero, focus attention initially toward moving forward by one unit. From here, moving upward by one unit satisfies the preliminary conditions and stays within the established numeric range. Similarly, moving downward by one unit to -1 or forward horizontally along the same line also remains within these acceptable limits. Thus, from this initial point of zero, three possible pathways or movement options emerge within a unidirectional, one-dimensional grid. The framework is structured around two preliminary premises: first, selecting zero as the initial point; and second, deciding whether or not to move from this point. Among the three initial numbers, zero is specified, forming—in a binary sense—a zero-dimensional premise for movement represented by M or ~M (moved or not moved). If the option of no movement (or zero movement) from the initial starting point is included, this introduces four initial options, rather than three if it is excluded. Considering whether to include or exclude this zero-movement scenario clarifies the context of subsequent analysis.

Applying the same consideration to starting points at 1 or -1 reveals that these positions are less agile compared to zero. Given the limitation of only two options for displacement from either of these points in a unidirectional grid—or four options in a bidirectional scenario—the median ratio of agility is 3:2 for the zero-position compared to either 1 or -1 in a unidirectional context, and 6:4 in a bidirectional scenario. For example, moving one unit forward or downward from position one is possible, as moving one unit upward or one unit forward from -1. Both these scenarios double their available options from two to four when bidirectional movement is allowed. Within this numeric framework, including the zero-movement option yields a total of 3 + 2 + 2 + 1 = 8 possible options, while excluding zero movement reduces this total to 7. For the bidirectional case, the inclusion of zero movement provides 6 + 4 + 4 + 1 = 15 possible options, and excluding it results in 14 options. To further clarify this conceptual development visually, Figure 1 illustrates the progressive expansion of directional movement options originating from a central starting point. This diagram depicts incremental increases in connectivity as the number of intervals grows outward from the initial triadic configuration toward increasingly complex, multi-directional structures. The top series of diagrams demonstrates the stepwise growth in available pathways at each incremental stage. In contrast, the bottom series further elaborates on this expansion by systematically extending possible movements across multiple intervals. The points depicted in Figure 1 are interconnected by radiating lines that represent all potential directional movements at each stage, visually emphasizing the exponential growth in complexity and connectivity inherent within interval-based numeric systems.

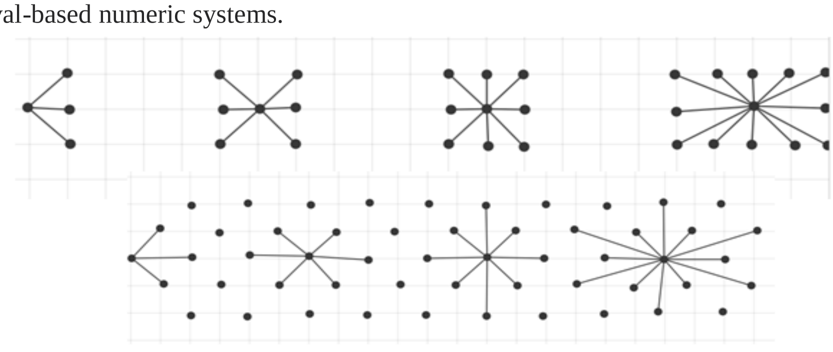

Figure 1: Progressive Expansion of Movement Options from Central Point

The first premise declares a numeric range from -1 to 1, while the second premise limits the analysis to three integers: 1, 0, and -1. For simplicity, the system begins with a single initial point, progressively building upon this foundation as the concept evolves. Starting with zero as the initial point, there are three options available for the first internal unit. Moving to the second interval, the endpoints 1 and -1 each contribute two additional options, and zero adds another three, thus totaling seven options for the second interval. When the no-movement option is included, the combined total for the two intervals becomes 3 (initial interval) + 1 (no movement) + 7 (second interval), resulting in a total of 11 options. Excluding the no-movement option reduces this number to 10, with endpoints further considered, whether clean-cut or truncated. To illustrate, starting with two points—zero along with either one or -1—yields five options: three originating from zero, and two from the second point (1 or -1). If all three integers (1, 0, 1) are included, seven options become available. Endpoints must be evaluated similarly: eliminating either endpoint 1 or -1 leaves five options (three from zero, plus two from the remaining integer). If both 1 and -1 are removed and only zero remains, three options persist. Conversely, removing zero and leaving only 1 and -1 provides four options, two from each integer, available in a unidirectional context. To systematically measure and analyze this numeric system, two key variables are defined: "a," representing the initial optional count, and "c," representing the endpoint optional count. Using these variables, the algebraic equations that capture the numeric relationships are as follows: "8(n - 1) + (a + c)" applies when including the no-movement option, while "7(n - 1) + (a + c)" applies when excluding it. For the simplest scenario (n = 1), including the no-movement option yields "4 + c," and excluding it yields "3 + c," ensuring the initial point is correctly represented. For all subsequent cases where n > 1, the equations are consistently applied: "8(n - 1) + (a + c)" (including no movement) and "7(n - 1) + (a + c)" (excluding no movement). Establishing a baseline, values such as "a = 0" and "c = 0" represent seamless intervals, whereas endpoint values, such as "c = 3" or "c = 5", reflect truncations of interval limits.

As a specific example, substituting n = 7 into the equation excluding the no-movement option, we have "7 × 6 + (a + c) = 42 + (a + c)." This generates the following numeric outcomes: 42 + 3 = 45; 42 + 3 + 3 = 48; 42 + 4 = 46; 42 + 3 + 4 = 49; 42 + 4 + 4 = 50; 42 + 5 = 47; 42 + 5 + 3 = 50; 42 + 4 + 5 = 51; and 42 + 5 + 5 = 52. Likewise, substituting n = 7 into the equation including the no-movement option, "8(n - 1) + (a + c)," results in "8 × 6 = 48," yielding subsequent calculations: 48 + 3 = 51; 48 + 3 + 3 = 54; 48 + 3 + 4 = 55; 48 + 4 + 4 = 56; 48 + 3 + 5 = 56; 48 + 5 + 4 = 57; and 48 + 5 + 5 = 58.

Define two key variables to measure this system:
a: the initial optional count
c: the endpoint, optional count
The Algebraic equations of the two formulas mentioned above:

- 8(n - 1) + (a + c) (including the no-movement option)
- 7(n - 1) + (a + c) (excluding the no-movement option)

For n = 1:

- Including the no-movement option: 4 + c
- Excluding the no-movement option: 3 + c
- Ensure the initial point is correctly represented.

For n > 1, apply the equations:

- 8(n - 1) + (a + c) (including no movement)
- 7(n - 1) + (a + c) (excluding no movement)

Include a = 0 and c = 0 as a baseline option—a seamless cutting at the limit of the nth interval—and values of 3 or 5 for c to reflect truncation of interval limits.

Substitute n = 7 into the equation 7(n - 1) + (a + c) (excluding the no-movement option):
7 × 6 + (a + c) = 42 + (a + c)
Calculations:

- 42 + 3 = 45
- 42 + 3 + 3 = 48
- 42 + 4 = 46
- 42 + 3 + 4 = 49
- 42 + 4 + 4 = 50
- 42 + 5 = 47
- 42 + 5 + 3 = 50
- 42 + 4 + 5 = 51
- 42 + 5 + 5 = 52

For the equation including the no-movement option, 8(n - 1) + (a + c) with n = 7:
8 × 6 = 48, then:

- 48 + 3 = 51
- 48 + 3 + 3 = 54

- 48 + 3 + 4 = 55
- 48 + 4 + 4 = 56
- 48 + 3 + 5 = 56
- 48 + 5 + 4 = 57
- 48 + 5 + 5 = 58

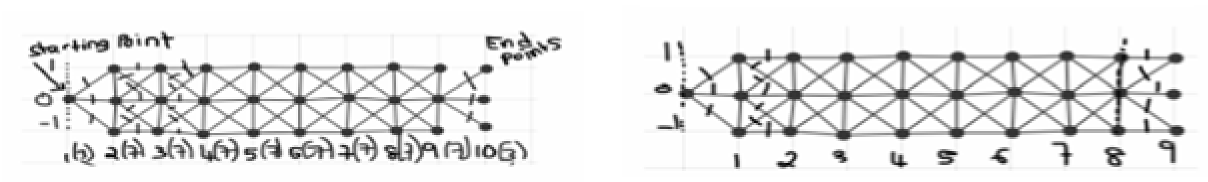

Figure 2: Visualization of Interval-Based Numeric Movement Grid

Figure 2 presents a structured numeric movement grid, visually illustrating directional and positional relationships based on a numeric range of (-1, 0, 1). The diagram distinctly marks the starting point at zero and extends horizontally across identified intervals from 1 through 9. At each interval, points are vertically positioned at -1, 0, and +1, interconnected by diagonal and horizontal line segments that vividly depict possible movement pathways. The figure differentiates between the starting point ("Starting Point") and the endpoints ("End Points") and includes numeric labels along the intervals to demonstrate sequential progression. Additionally, each subfigure employs variations in color and contrast to enhance clarity and visual accessibility, reinforcing the viewer's comprehension of structural connections and movement options across intervals. To better understand and analyze the numeric relationships and behaviors represented in Figure 2, it is helpful to apply a systematic analysis of ratios and their reciprocals. Employing a harmonic analysis approach provides valuable bidirectional insights and a more comprehensive, spherical perspective on numeric interconnections. Constructing a table to illustrate all derived values and their corresponding ratios from these outputs further supports this detailed examination.

Additionally, an analysis of the original inputs and their function ratios helps uncover embedded, multi-tiered numeric relationships. To illustrate these numeric relationships, Table 1 below summarizes interval growth and cumulative movement options, distinguishing scenarios that include or exclude the no-movement option. The table carefully outlines interval growth, cumulative sums across intervals, and details distinct cases for base endpoints and truncated intervals (with values of c = 0, 3, or 5). Structured rows represent interval sequences (n), increments within each interval, and cumulative totals, thus providing a comprehensive numeric reference to effectively analyzing the patterns and relationships inherent within the interval-based numeric system.

Table 1: Interval Growth and Cumulative Movement Options (Including and Excluding No-Movement Option)

n	Interval Growth (Including)	Interval Growth (Excluding)	Sum of Intervals (Including)	Sum of Intervals (Including)	Sum of Intervals (Excluding)	Sum of Intervals (Excluding)	Base Value (Including) c = 0	c = 3 (Including)	c = 5 (Including)	Base Value (Excluding) c = 0	c = 3 (Excluding)	c = 5 (Excluding)
1	4	3	4	4	3 (3)	3 (3)	4	7	9	3	6	8
2	8	7	4 + 8 = 12	4 + 8 = 12	3 + 7 = 10	3 + 7 = 10	12	15	17	10	13	15
3	8	7	4 + 8 + 8 = 20	12 + 8 = 20	3 + 7 + 7 = 17	10 + 7 = 17	20	23	25	17	20	22
4	8	7	4 + 8 + 8 + 8 = 28	20 + 8 = 28	3 + 7 + 7 + 7 = 24	17 + 7 = 24	28	31	33	24	27	29
5	8	7	4 + 8 + 8 + 8 + 8 = 36	28 + 8 = 36	3 + 7 + 7 + 7 + 7 = 31	24 + 7 = 31	36	39	41	31	34	36
6	8	7	4 + 8 + 8 + 8 + 8 + 8 = 44	36 + 8 = 44	3 + 7 + 7 + 7 + 7 + 7 = 38	31 + 7 = 38	44	47	49	38	41	43

7	8	7	4 + 8 + 8 + 8 + 8 + 8 + 8 = 52	44 + 8 = 52	3 + 7 + 7 + 7 + 7 + 7 + 7 = 45	38 + 7 = 45	52	55	57	45	48	50
8	8	7	4 + 8 + 8 + 8 + 8 + 8 + 8 + 8 = 60	52 + 8 = 60	3 + 7 + 7 + 7 + 7 + 7 + 7 + 7 = 52	45 + 7 = 52	60	63	65	52	55	57
9	8	7	4 + 8 + 8 + 8 + 8 + 8 + 8 + 8 + 8 = 68	60 + 8 = 68	3 + 7 + 7 + 7 + 7 + 7 + 7 + 7 + 7 = 59	52 + 7 = 59	68	71	73	59	62	64
10	8	7	4 + 8 + 8 + 8 + 8 + 8 + 8 + 8 + 8 + 8 = 76	68 + 8 = 76	3 + 7 + 7 + 7 + 7 + 7 + 7 + 7 + 7 + 7 = 66	59 + 7 = 66	76	79	81	66	69	71

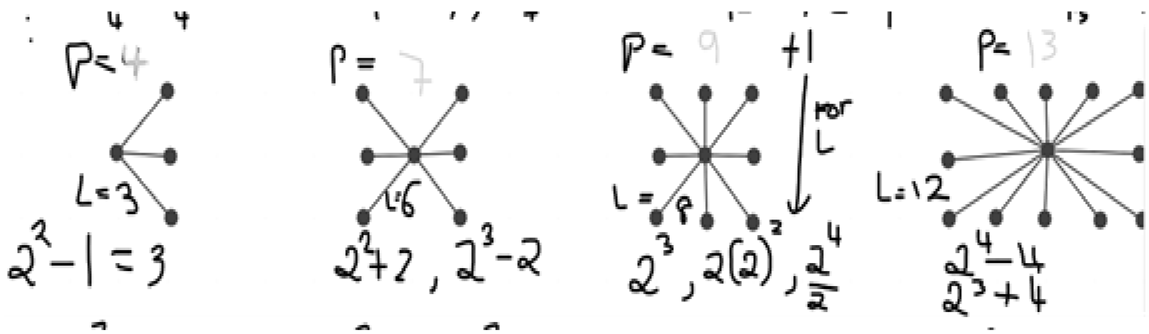

Figure 3: Mathematical Relationship between Points (P) and Lines (L) in Interval Expansion

Figure 3 illustrates the mathematical relationships that exist between points (P) and connecting lines (L) within progressively expanding interval systems. Each subfigure displays points radiating outward from a central node, labeled with numeric notations that highlight their algebraic relationships. The formulas provided beneath each graphical representation vividly demonstrate numeric patterns, such as exponential relationships (for instance, powers of 2), additive adjustments (plus or minus numeric increments), and fractional increments. These formulas clarify the structural logic that governs point-to-line ratios, connecting numeric configurations with their corresponding algebraic representations. Thus, the visualization demonstrates how points and lines systematically increase in complexity through well-defined mathematical relationships as intervals continue to expand.

To provide further numeric insight, initial comparison values derived from earlier equations, specifically the numbers 42 and 48, are established before applying any truncations or extensions within the numeric function. Dividing 42 by 48 yields a ratio of 0.875, equivalent to 7/8, showing that the relationship is characterized by a difference of precisely 1/8 (0.125). Taking the reciprocal of this ratio (48 divided by 42) results in approximately 1.14285714, equivalent to the fractional ratio of 8/7, and dividing this reciprocal quotient by four yields 0.285714, a numeric value of particular significance due to its recurring presence in various mathematical sequences. For instance, 19 multiplied by 6 equals 114; similarly, 6 divided by 7 equals 0.857142857, while seven divided by 6 equals 1.166666667. Multiplying 19 by 15 results in 285; adding the fraction 5 ÷ 7 produces precisely 285.714285. Then, adding 285 and 15 equals 300.

Further numerical exploration reveals that dividing 19 by 48 produces an intriguing numerical pattern, equal to 0.395833333. Thus, the number 19 functions effectively as a numeric base within the dynamics of the 8/7 and 7/8 ratios, instrumentalizing the fractional ratio 1/7 and providing precise, pragmatic numeric control at any desired decimal scale. This phenomenon can be vividly illustrated in structured numeric tables, demonstrating that seemingly daunting mechanical computations can be made intuitive and highly customizable. For example, calculating 2 ÷ seven yields the repeating decimal 0.285714285, which relates directly to multiples of 19 multiplied by 15. Similarly, adding multiples of 19 × 15 plus fractional increments, such as 4 ÷ 7, equals 286 minus 3 ÷ 7. Likewise, the numeric value 114 (or 1.14) aligns with multiples of 19, as 19 × 6 equals 114; adding 2 ÷ 7 results in 114.285714285. Since 1.14 equals 0.19 multiplied by 6, systematic fractional increments of 0.002 ÷ 7 can be applied, demonstrating a calibration method that eliminates ambiguity around decimals and fractions, providing transparent numeric access.

Additionally, recognizing that 8 ÷ 7 equals 1.14285714 underscores the invariant numeric relationships embedded within this numeric framework. This consistent numeric base and grid is deliberately engineered for use, allowing the structured numeric system to function both universally and elegantly. Therefore, analyzing the initial equations and output variations centers the numeric data around the values 42 and 48, reflecting a fundamental relationship (7 - 1 = 6) that is expressly aligned with the structured numeric limits observed consistently. These numeric outputs form intriguing pairs that transcend simple numeric relationships, manifesting harmonic sequences that function effectively as mathematical sculpting mechanisms.

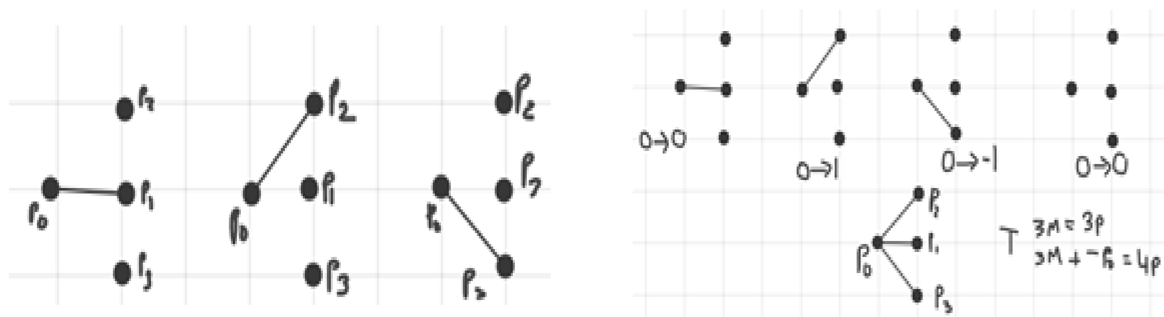

Figure 4: Pathways and Movement Options from Initial Point p_0

Figure 4 illustrates various directional pathways and positional outcomes originating from the initial reference point labeled p_0. The diagram demonstrates multiple possible movement scenarios starting from the origin (0), including horizontal and diagonal moves toward subsequent points labeled p_1, p_2, and p_3. Specific directional movements are typically marked, including "0 → 0," indicating no vertical movement from the initial point; "0 → 1," representing upward vertical movement; and "0 → -1," representing downward vertical movement. Additionally, the figure provides algebraic equations that demonstrate numeric relationships between movements (M) and points (P), such as "3M = 3P," ly indicating three movements corresponding directly to three points, and "3M + P_0 = 4P," suggesting that including the initial point p_0 increases the total count of points to four.

This visualization shows how various combinations of directional movements and positions systematically expand from an initial state, reflecting the underlying combinational logic of numeric intervals. To visually illustrate the concept, Figure 4 displays four distinct dots labeled p_0, p_1, p_2, and p_3. The initial point, p_0, occupies the zero position within the ly defined numeric range of -1 to 1. From this initial point, three subsequent points illustrate one-unit forward movements: p_1 represents forward movement without vertical displacement; p_2 represents forward movement with an upward vertical shift of one unit; and p_3 represents forward movement combined with a downward vertical change of one unit. The diagram thus concretely depicts the initial triadic movements and pathways previously discussed. Each dot.ly marks a distinct positional outcome, with connecting line segments visually illustrating specific directional shifts during these movements.

Furthermore, Figure 4 presents all possible outcomes originating from the initial point p_0. These include a shift from "0 to 0," representing no vertical movement; "0 to 1," representing a one-unit upward movement; "0 to -1," representing a one-unit downward movement; as well as considering the possibility of no movement at all. The total set of outcomes, expressly denoted as T, encompasses these three directional movements and four positional outcomes, including the option to remain stationary. Figure 3 previously illustrated the complete set of potential options and outcomes for the numeric values—0, 1, and -1—representing their respective movements and resulting positions within the established numeric parameters. Each directional possibility and its resulting outcome remain constrained by the foundational numeric limits previously established.

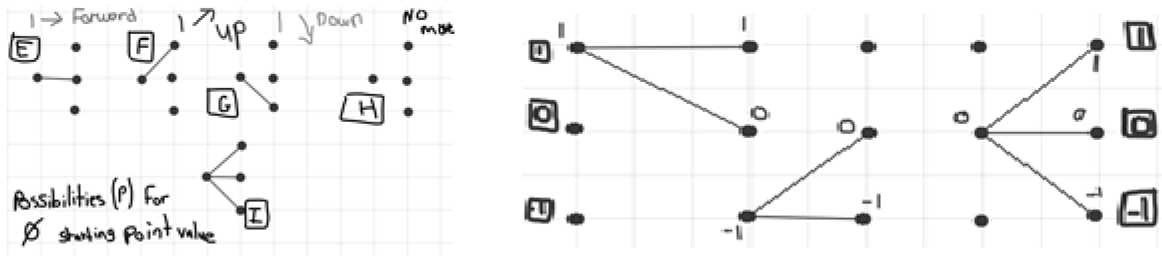

Figure 5: Directional Movements and Possible Outcomes from Starting Point Zero

Figure 5 illustrates the directional movements and corresponding possible outcomes, starting from an initial point defined as zero. The figure demonstrates all potential directional movements, including forward movement (to the right), upward movement, downward movement, as well as considering the scenario of no movement at all. Each potential directional choice is distinctly marked alongside its specific numeric outcomes, such as forward movements labeled as "1 → Forward," vertical movements labeled as "1 → Up" and "1 → Down," and stationary positions are identified as "No move."

Additionally, the diagram ly indicates multiple positional possibilities (P) originating from the initial zero point (∅), labeling specific points as E, F, G, H, and I. Numeric relationships and positional outcomes, specifically the numeric values (1, 0, and -1), are also ly marked along the right-hand side of the diagram. This visual representation systematically highlights the numeric options resulting directly from the specified directional movements. Thus, this comprehensive visualization provides enhanced clarity regarding how various directional choices directly influence numeric outcomes within the structured interval-based grid system.

FOUNDATIONAL MATHEMATICS AND COMPUTATIONAL LITERACY

This foundational mathematics exploration aims to provide a detailed, fiber-like understanding of both the structure and the underlying system of numeric relationships. By defining numeric intervals, directional options, and positional outcomes, the mathematical framework establishes a visualization of interconnected fibers and threads, each representing distinct numeric pathways and combinational relationships. Crucially, adjustments to the "weights" or emphasis placed upon these numeric relationships impact computational outcomes, influencing the structure, connectivity, and resulting behaviors within computational logic systems.

In the context of critical literacy, particularly in our current age marked by widespread disinformation and increasingly invasive technologies—such structured numeric understanding becomes essential. By offering precise, fiberistic detail on numeric relationships, interval pathways, and the weight distributions underlying computational processes, this approach significantly enhances one's ability to access, interpret, and critically analyze deeply embedded numeric ratios and dynamics.

Explicit awareness of how numeric weights and distributions implicitly shape computational outcomes provides a powerful tool for critical engagement and literacy. This numerically structured approach equips readers with the necessary clarity and insight to decipher computational logic and algorithmic structures, offering enhanced access and capacity to discern both overt and subtle numeric manipulations. Thus, it empowers individuals to navigate and critically engage with the implicit dynamics and numeric ratios at play in complex computational systems and algorithmic frameworks, fostering a more profound understanding and informed engagement in a technology-driven informational landscape.

The foundational mathematics described above provides a structured numeric understanding crucial for critical literacy, particularly within a digital landscape increasingly dominated by AI-generated content. The clarity and neatness inherent in AI-written texts, characterized by highly assertive and declarative statements, result directly from algorithmic logic built upon precisely defined numeric intervals, directional pathways, and weighted distributions. Such numeric frameworks inherently shape AI-generated outputs, producing content that mimics natural assertiveness and clarity, thereby enhancing its persuasive power.

Detecting AI-generated content must, therefore, extend beyond simplistic watermarking or superficial stylistic markers. Advanced detection requires recognizing subtle numeric and logical signatures embedded deeply within the structural logic and premise-based reasoning of AI-generated texts. Specifically, it involves identifying numeric weight distributions, directional logic, and combinational premises that algorithmically construct seemingly organic but systematically designed narratives.

This numeric and logical structuring is especially critical within the context of systemic and widespread disinformation campaigns. These campaigns leverage algorithmically generated content to exploit echo-chamber dynamics, strategically amplifying certain viewpoints while suppressing others. Thus, critical literacy and detection strategies must primarily focus on identifying the numeric logic, structured algorithmic patterns, and declarative assertiveness characteristic of AI-generated narratives, rather than relying solely on superficial indicators.

Through this numeric approach, critical literacy becomes not merely about identifying disinformation but also about understanding how numeric logic and structured computational reasoning shape narrative construction. This understanding empowers individuals to critically assess algorithmically driven discourse, effectively navigating the pervasive, systematically structured, and numerically engineered landscape of modern information.

Practical Application and Numeric Mapping of Logical Premises through Fibristic Epistemology

In bridging theory to practical application, the current analysis leverages logical premises detailed in peer-reviewed research. Studies conducted by Bouattoura (2025a) systematically identified structural and logical biases within stakeholder reports by applying rigorous numeric ratio analyses and mapping techniques within the context of the Algerian Universal Periodic Review Stakeholders' Summary Report. Additionally, the present research adopts a fibristic epistemological approach, aligning closely with the methodological framework defined by Bouattoura (2025b), which prioritizes precision, transparency, and accountability when examining numerical structures. Such fibristic methodology emphasizes detail and deterministic logic rather than qualitative interpretations or inferred conclusions, following a Mohandese style—precise, systematic, and fully accountable (Bouattoura, 2025b).

As previously stated, the guided question for the research remains:

"How can numeric logic and directional analysis, informed by fibristic epistemology, illuminate systemic biases and engineered structures within complex informational constructs?"

The detailed mathematical and directional analyses presented earlier were necessary precisely to equip readers with an intellectual understanding of numeric frameworks and directional grids. Such foundational knowledge enables readers to accurately recognize and critically evaluate structured biases and engineered logic embedded within complex informational systems.

Table 2: Numeric Ratio Distribution Across Three Levels (Level 1, Level 2, Nested) for Statements 2–64				**Table 3: Derived Row and Column Positions Corresponding to Numeric Ratios**					
Statement Number	Level 1	Level 2	Nested	Level1 R	Level 2R	Nested R	Level1 C	Level 2C	Nested C
2	0.375	0.5	0.625	8	2	8	6	7	8
3	0.181818	0.545455	0.636364	11	11	8	3	7	11
4	0.333333	0.666667	0.666667	3	7	3	6	3	7
5	0.666667	0.333333	0.333333	3	6	3	7	3	6
6	1	0	0	1	6	1	7	1	6
7	0.444444	0.555556	0.555556	9	9	7	6	7	9
8	0.428571	0.428571	0.571429	6	7	7	7	6	7
9	0.666667	0.333333	0.333333	3	6	3	7	3	6
10	0.3	0.7	0.7	10	10	9	5	9	10
11	1	0	0	1	6	1	7	1	6
12	1	0	0	1	6	1	7	1	6
13	0.6	0.4	0.4	5	5	6	7	6	5
14	0.5	0.5	0.5	7	2	7	2	7	2
15	0.666667	0.333333	0.333333	3	6	3	7	3	6
16	1	0	0	1	6	1	7	1	6
17	0.333333	0.416667	0.666667	3	6	3	6	12	7

18	0.5	0.5	0.5	7	2	7	2	7	2
19	1	0	0	1	6	1	7	1	6
20	1	0	0	1	6	1	7	1	6
21	1	0	0	1	6	1	7	1	6
22	0.666667	0.333333	0.333333	3	6	3	7	3	6
23	0.4	0.4	0.6	6	5	5	5	6	7
24	0.5	0.5	0.5	7	2	7	2	7	2
25	0.5	0.5	0.5	7	2	7	2	7	2
26	0.571429	0.428571	0.428571	7	7	6	7	6	7
27	0.625	0.375	0.375	8	6	8	8	8	6
28	0.333333	0.666667	0.666667	3	7	3	6	3	7
29	0.666667	0.333333	0.333333	3	6	3	7	3	6
30	0.833333	0.166667	0.166667	6	6	5	9	5	6
31	0.5	0.25	0.5	7	4	7	2	6	2
32	0.333333	0.333333	0.666667	3	6	3	6	3	7
33	1	0	0	1	6	1	7	1	6
34	0.375	0.375	0.625	8	6	8	6	8	8
35	0.6	0.2	0.4	5	5	6	7	5	5
36	1	0	0	1	6	1	7	1	6
37	1	0	0	1	6	1	7	1	6
38	0.5	0.5	0.5	7	2	7	2	7	2
39	0.666667	0.333333	0.333333	3	6	3	7	3	6
40	0.5	0.375	0.5	7	6	7	2	8	2
41	0.666667	0.333333	0.333333	3	6	3	7	3	6
42	1	0	0	1	6	1	7	1	6
43	0.428571	0.428571	0.571429	6	7	7	7	6	7
44	0.571429	0.285714	0.428571	7	7	6	7	5	7
45	0.6	0.2	0.4	5	5	6	7	5	5
46	0.5	0.25	0.5	7	4	7	2	6	2
47	0.5	0.5	0.5	7	2	7	2	7	2
48	0.75	0.25	0.25	4	4	6	9	6	4
49	0.6	0.2	0.4	5	5	6	7	5	5
50	0.571429	0.285714	0.428571	7	7	6	7	5	7
51	0.666667	0.166667	0.333333	3	6	3	7	5	6
52	0.666667	0.333333	0.333333	3	6	3	7	3	6
53	0.571429	0.428571	0.428571	7	7	6	7	6	7
54	0.5	0.333333	0.5	7	6	7	2	3	2
55	1	0	0	1	6	1	7	1	6
56	0.428571	0.428571	0.571429	6	7	7	7	6	7
57	0.75	0.25	0.25	4	4	6	9	6	4
58	0.5	0.375	0.5	7	6	7	2	8	2

59	0.375	0.5	0.625	8	2	8	6	7	8
60	0.666667	0.333333	0.333333	3	6	3	7	3	6
61	0.666667	0.333333	0.333333	3	6	3	7	3	6
62	0.8	0.2	0.2	5	5	5	8	5	5
63	0.5	0.375	0.5	7	6	7	2	8	2
64	0.6	0.2	0.4	5	5	6	7	5	5

The numeric ratio analysis began with the precise assignment of fractional values to each statement across three levels—Level 1, Level 2, and Nested(see Table 2). Table 2 provides the detailed numeric ratios assigned to each statement (numbered 2 through 64) across three logical premise levels: Level 1, Level 2, and Nested. These numeric ratios represent the precise weighting of logical premises used in the analysis, independent of any geometric or structural frameworks.

Table 3 presents the row (R) and column (C) coordinates derived from translating each numeric ratio from Table 2 into positional locations. Specific numeric coordinates represent each statement within three logical levels (Level 1, Level 2, and Nested), specifying its location within a structured numeric array. These derived coordinates provide the basis for subsequent visualization and pattern analysis. Each assigned numeric ratio was carefully matched with specific numeric positions within the structured Farid–El Djezairi triangle, arranged in rows and columns numbered from 0 to 14. To accurately translate each ratio into coordinates, the numeric value was located within the triangle by comparing it directly to the incremental fractions in each row, thus deriving a precise column position based on the closest numeric match.

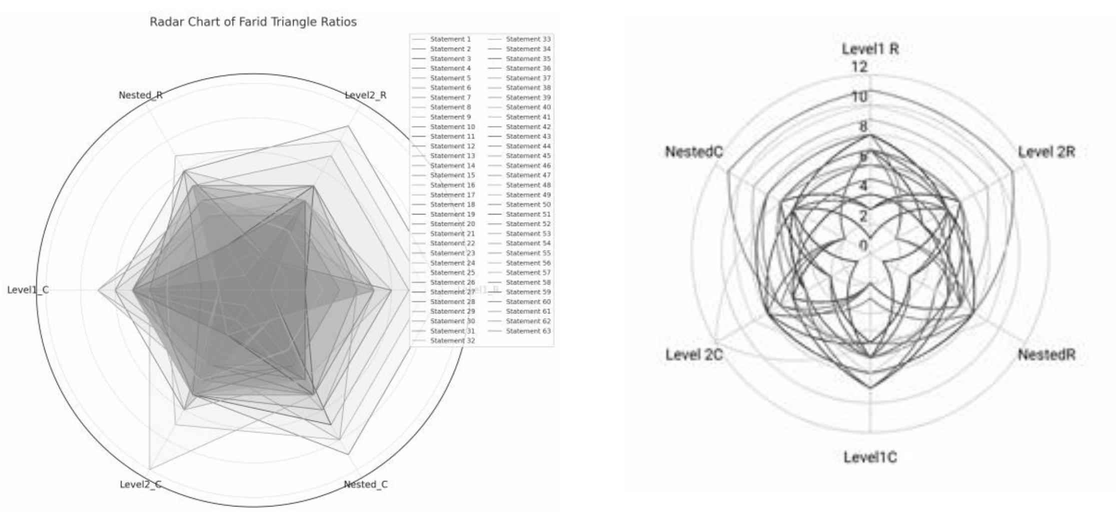

Figure 6: Radar Chart Visualization of Numeric Ratios Mapped onto the Farid–El Djezairi Triangle

Figure 6 visualizes the numeric ratios previously defined (Table 2) after they have been translated into precise numeric positions (Table 3) within the Farid–El Djezairi triangular framework. Each plotted line represents a specific numeric statement (Statements 2–64), with positional coordinates displayed along axes labeled Level1_R, Level2_R, Nested_R, Level1_C, Level2_C, and Nested_C. Distinct and consistent intersections within the radar plot indicate systematic numeric alignments, forming structured geometric patterns, particularly hexagonal and hexagram configurations. These repeating geometric patterns demonstrate the numeric logic, directional structuring, and engineered numeric bias embedded within the original logical premises, providing visual evidence of systematic numeric design rather than naturally or randomly occurring data. Upon systematically examining these derived positions, a deterministic and deliberate numeric pattern emerged: the majority of Level 1 and Level 2 numeric positions aligned distinctly with the 7th column of the triangle, while the Nested level numeric values were predominantly aligned with columns positioned differently. Such intentional alignment reveals an engineered structure rather than organic or randomly discrete data points. Specifically, the numeric positioning within the 7th column strongly suggests an intentional numeric bias and structural directionality—mirroring known geometric ratios, such as the vertex-to-edge ratio in a cube (8 vertices to 12 edges, precisely a 2/3 ratio), inherently directional and structurally biased.

Furthermore, plotting these coordinates onto a radar chart (as seen in Figure 6), geometric intersections emerged, distinctly forming consistent hexagonal and hexagram patterns. The repeated and consistent nature of these patterns visually confirms that the numeric logic governing the original language and premises in the analyzed text was engineered and systematically biased, designed to appear natural while reinforcing targeted numeric structures. This numerical evidence, revealed through the Farid–El Djezairi triangular framework, provides proof that the underlying logic of the original material was intentionally structured, widespread, and systematically directional. Moreover, readers are directed to Appendix C: Planar Numeric Ratio Visualization and Positional Mapping, which reveals even deeper numeric relationships extending beyond the previously identified hexagonal and hexagram configurations. Specifically, when conducting numeric visualization using Google Sheets' built-in radar chart application, the initial plotting based on a structured numeric framework (rows as statements, columns as numeric levels, and nested positions) yields consistent hexagonal and hexagram configurations. However, when utilizing Google Sheets' "switch rows and columns" function—essentially transposing the dataset—the numeric relationships undergo a meaningful positional realignment. Such transposition systematically shifts the visual orientation, revealing previously obscured numeric relationships and highlighting pentagonal and pentagram shapes instead of the original hex-based geometries.

The emergence of these pentagonal geometries introduces the numerical ratios of 5/6 and 6/5, directly stemming from this relational transposition. The appearance of pentagonal and pentagram configurations through the transposition of rows to columns and columns to rows underscores a deeper numeric flexibility embedded within the structured dataset, which is dependent precisely upon analytic framing and positional arrangement. Thus, the robustness of the numeric system is confirmed by its ability to systematically produce distinct geometric configurations—hexagonal and hexagram in one analytic frame, and pentagonal and pentagram in its transposed counterpart—demonstrating an inherent numeric duality and engineered structural coherence underlying the dataset.

Explicit Transformation Of A 3D Cube Into A 2D Hexagram Via Diagonal Projection

Having demonstrated evidence of numeric logic and deliberate structural bias through the mapping of numeric ratios onto the Farid–El Djezairi triangle, we now visually illustrate and confirm these geometric relationships through a geometric transformation. Specifically, we begin by defining a cube in three-dimensional space, using coordinates along the x, y, and z axes, specifically placing points at (-1, -1, -1), (1, -1, -1), (1, 1, -1), (-1, 1, -1), (-1, -1, 1), (1, -1, 1), (1, 1, 1), and (-1, 1, 1). Next, select a diagonal viewing angle—from the corner at (-1, -1, -1) directly toward the opposite corner at (1, 1, 1). To visualize this in two dimensions, apply a mathematical projection defined by two equations:

$$2D\_x = y - x$$
$$2D\_y = z - x$$

Applying these equations collapses the 3D points onto a 2D plane. Each of the cube's original points translates directly into positions in 2D space: Point 1 (origin) becomes (0,0), Point 2 becomes (-2,0), Points 3 and 5 overlap at (0,2), Point 4 at (2,2), Point 6 at (-2,2), Point 7 at (0,4), and Point 8 at (2,4). Due to this projection, specific points overlap, and intersections occur. By connecting every point to every other point on this 2D plane, multiple symmetrical intersections emerge, visually forming the distinct shape of a hexagram. Thus, through definition, diagonal viewpoint selection, mathematical projection, and complete point-to-point connection, the original 3D numeric structure visually transforms into the recognizable hexagram shape in 2D space, as illustrated in Figure 7. Figure 7 depicts the complete connectivity and intersection points of a cube projected onto a 2D plane from a diagonal viewpoint. Each of the eight corners of the cube is connected to every other corner, forming multiple symmetrical intersection points. These intersections visually manifest as a well-defined hexagram, illustrating the underlying numeric logic and structured relationships inherent in the original three-dimensional cubic structure.

As displayed above (Figure 7a) and visualized interactively via Desmos (https://www.desmos.com/3d/ldubxlc0iv), the linear plane equations $x + y = z$ and their geometric reflections effectively translate the three-dimensional cubic relationships into two-dimensional representations. Figure 7a illustrates these planar equations and their intersections, confirming the consistency and structural integrity of the numeric logic when visualized. The transformation provides an intuitive and systematic approach to visualizing numeric logic through structural geometry, thereby reinforcing the direct connection between geometric representation and numeric structure. Furthermore, this geometric representation illustrates the reverse-engineering process—structurally decoding complex three-dimensional relationships into simpler two-dimensional forms—and aligns closely with the base-two systems fundamental to octal and hexadecimal numbering, key numerical languages in computer science.

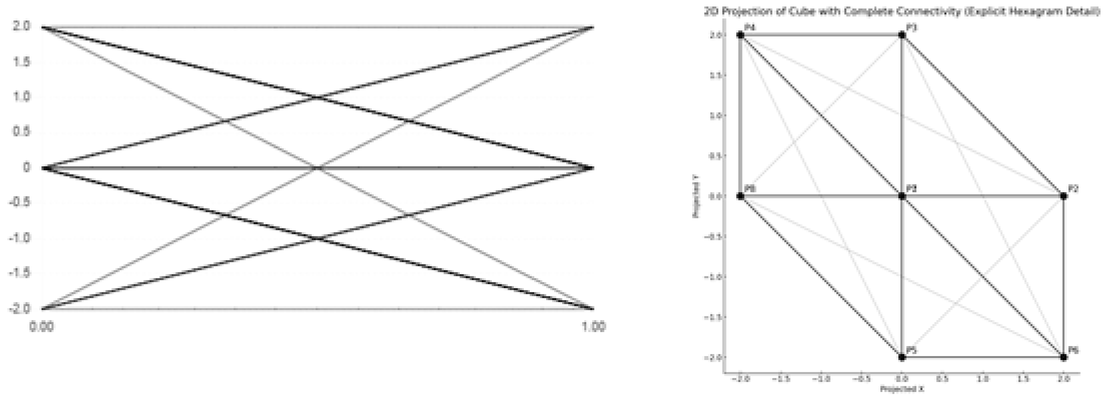

Figure 7: 2D Projection of a Fully Connected 3D Cube Forming a Hexagram

Figure 7a: *Visualization of the 3D-to-2D Geometric Transformation: Planar Slices of a Cube Defined by Linear Equations and Their Symmetrical Reflections Projecting into a Hexagram*

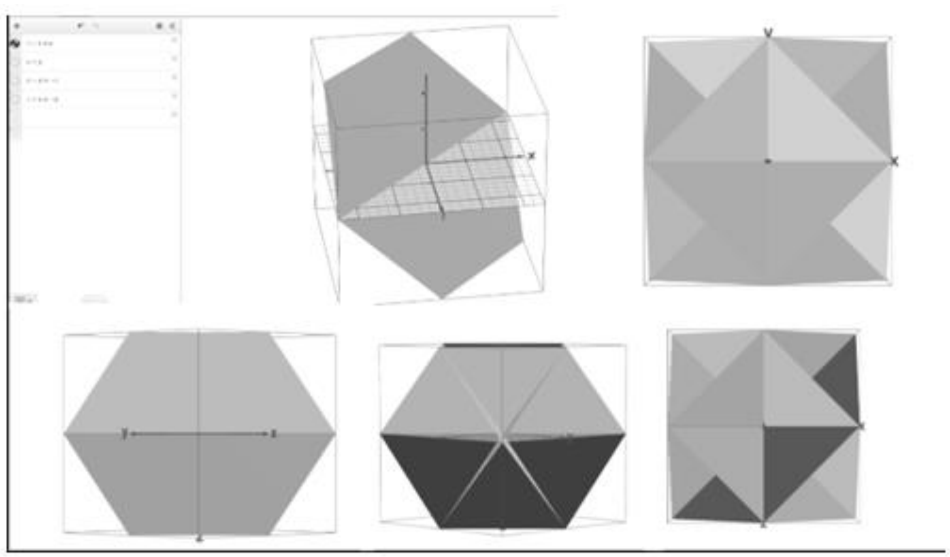

Figure 8: Comparative Visualization (Scatter and Area Charts) of Numeric Positions Derived from Logical Premise Ratios

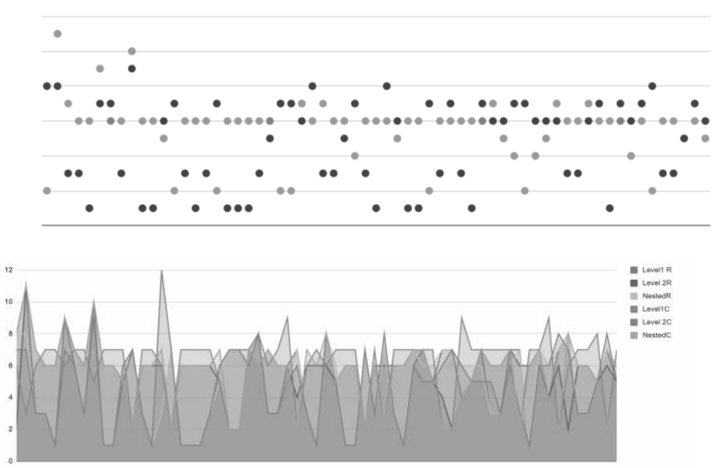

Figure 8 combines two distinct visual representations (a scatter plot and an area chart) of the numeric positions derived from the logical premise ratios (Table 3). The scatter plot (top) visually highlights the numeric coordinates (rows and columns) assigned to each level across the various statements. The lower visualization (area chart) provides an additional perspective, demonstrating the numeric distributions and overlaps among levels. The highly structured numeric distribution evident in both charts strongly indicates that these numeric positions are not representative of naturally occurring or discretely measured data. Specifically, given that the original report document addresses concerns about translations and cultural synthesis—topics inherently subject to significant variability—one would expect considerable numeric and positional diversity. However, the distinct and recurring numeric alignments and structured patterns illustrated here underscore that the numeric logic governing these premises is intentionally engineered. The numeric structure does not reflect randomness or natural variability; instead, it reveals systematic numeric bias and inherent directionality embedded within the logical construction of the original text.

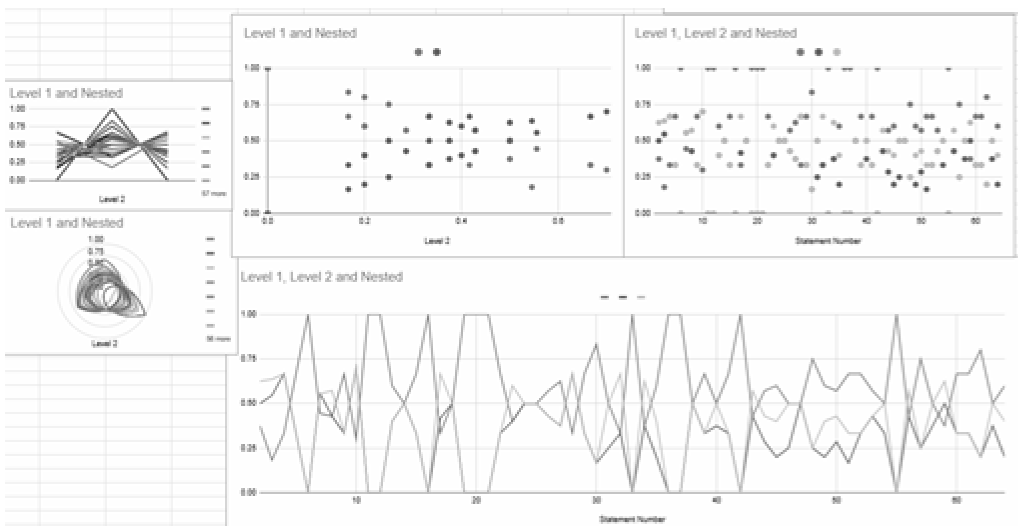

Figure 9: Cross-Validation Visualizations of Original Numeric Ratios

Figure 9 consists of five distinct graphical representations produced from the original numeric ratios (Table 2) using built-in computational methods aligned with modern analytical standards. The figure includes two radar-style plots, two scatter plots, and a line-chart representation, each constructed directly from raw ratio data without further positional translation. Across all five visualizations, distinct triangular and hexagonal patterns consistently emerge. Notably, the scatter plots exhibit an abnormal degree of symmetry and precision, suggesting a theoretical numeric structure rather than natural variability or randomness. Such symmetrical patterns strongly suggest the numeric data used in the original logical premises was deliberately engineered, reflecting intentional numeric design and bias rather than authentic, organically derived discrete data points. This cross-validation confirms earlier findings regarding the systematically structured nature of the numeric logic governing the original research document. Continuing the analysis of the numeric ratios presented in Table 2, the raw numeric data was examined through radar chart visualization techniques using Google Sheets. Each radar chart systematically compares the numeric ratios of Level 1, Level 2, and Nested premises, considering both direct and converse numeric relationships.

Through these comparisons, distinct and consistently repeating patterns began to emerge. Instead of producing scattered or irregular distributions expected from organically derived data, especially from a document addressing cultural and translation-based issues—these numeric visualizations display precise, repeating spirals and crescent shapes. Remarkably, these spiral patterns closely align with the numeric proportion's characteristic of the golden ratio, consistently clustering around numeric values between approximately 0.60 and 0.66, with a particular emphasis on a numeric alignment near 0.61. Such precise and repetitive numeric consistency strongly indicates a systematic, invariant numeric structure underlying the logical premises of the original document. These numeric alignments confirm that the original logic was intentionally structured, embedding numeric bias and directional relationships deliberately into the language and logical construction of the text. This numeric phenomenon becomes even more evident in the radar-based visualizations presented here in Figure 10.

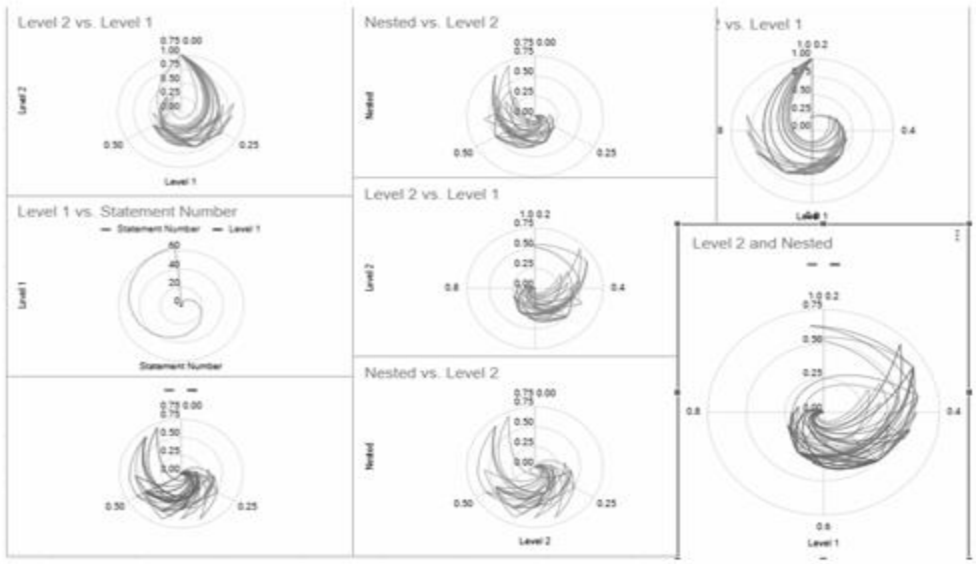

Figure 10: Radar Chart Comparative Analysis of Numeric Levels Revealing Systematic Golden Ratio Patterns

Figure 10 presents multiple radar charts generated through Google Sheets, systematically comparing numeric ratios across Level 1, Level 2, and Nested levels, including inverse comparisons. These visualizations consistently reveal well-defined spiral and crescent shapes, aligning closely with proportions near the golden ratio (approximately 0.61 and between 0.60 and 0.66). Such uniformity and precision illustrate an embedded numeric invariant within the logical framework, further supporting the conclusion that the numeric logic and structure governing the original document's premises are deliberately engineered and structurally biased rather than natural, organic, or discrete.

CONCLUSIONS AND IMPLICATIONS: FIBRISTIC ANALYSIS OF NUMERIC LOGIC AND SYSTEMIC BIAS

To conclude, the study builds upon Bouattoura's (2025a) examination of logical constructs and systemic biases in the Algerian Universal Periodic Review stakeholders' summary report. It is instrumented through the fibristic epistemological framework developed by Bouattoura (2025b). Additionally, it translates numeric analyses within the Farid–El Djezairi triangular structure (Bouattoura, 2025c). The core objective of the research was to scaffold complex jargon and mathematical notation, making detailed numeric and logical structures accessible to scholars from non-technological and non-mathematical backgrounds, as well as practitioners from various fields. The approach is intentionally undiscriminating; however, such scaffolding does not translate to facility or ease, as doing so would unequivocally go against the El Djezairi ethos and fibristic ethos approach.

The scope was to utilize the premises and arguments presented in an existing document and apply them to explain the mathematical and directional aspects, thereby helping readers intellectually grasp the directional grid. It demonstrates the 2/3 vertex-to-edge relationship and, through iterative processes, also reveals harmonic structures that create hexagonal and hexagram configurations. These structures facilitate the formulation of algorithms easily referenced by linear equations. Furthermore, the methodology employed involves truncation, which is directly tied to deterministic iterations and numerical frameworks. Future research will build upon the current understanding, further demonstrating the mathematical and technological accessibility that can be translated from this foundation.

The overarching 2/3 ratio, through repeated iterations, establishes a structural pattern fundamental to numeric logic. Moreover, the use of the Farid triangular structure and the ratios embedded within Algerian design and titling serve as strategic and invisible normalizers. Further demonstrates the deliberate, methodical, and systematic nature of the numeric logic and structured bias examined throughout the study. The implications are significant and necessitate deeper reflection; if such structured biases exist at the United Nations reporting level, it compels inquiry into their presence and influence in more accessible everyday communication platforms. There is thus an urgent need to heighten critical literacy and foster interdisciplinary collaboration to navigate and critically evaluate systematically engineered informational constructs. Additionally, similarities in numeric ratios between the Farid–El Djezairi triangular structure study by Bouattoura (2025c) and the initial logical premises dataset were recognized, prompting their application within the current logic study. Interestingly, the Farid–El Djezairi analysis revealed numeric orientations toward the .577 ratio and the golden ratio. Similarly, in this study, before any translations or positional mappings, the raw numeric ratios displayed the same orientations. Recognizing this numeric consistency motivated the decision to test and analyze the dataset in the first place. For more detailed numeric ratios, cross-validation visualizations, and comprehensive analyses that substantiate these findings, readers are referred to Appendix 1: Detailed Numeric Ratios and Cross-Validation Visualizations (Report-star.pdf). This supplementary material provides extensive numerical evidence and graphical representations, reinforcing the claims of systematic numerical structuring and engineered bias discussed throughout the main text.

DISCLOSURE ON THE USE OF AI IN EDITING AND FORMATTING

In preparing this article, artificial intelligence (AI) tools were utilized strictly for editing, formatting, and enhancing readability. Specifically, specialized AI platforms, including Academicia and Code Mentor—were employed to ensure clarity, grammatical accuracy, and adherence to APA formatting guidelines. Employing these AI tools aligns directly with the methodological transparency detailed in earlier research, which emphasizes critical literacy, democratic access, and the decolonization of knowledge frameworks through technology-enhanced platforms (Bouattoura, 2024). Consistent with the ethical principles articulated in "Overcoming Barriers with AI: Developing the El Djezairi Tool to Expose International Structural Inequalities through UPR Analysis" (Bouattoura, 2024), the current manuscript explicitly discloses the supportive role of AI. All conceptual and intellectual content remains exclusively the original work of the author, with AI tools serving only to improve presentation quality and coherence, thereby rigorously maintaining academic integrity throughout the research process.

REFERENCES

[1] Bouattoura, F. (2025a). Logical constructs and systemic biases in the Algerian UPR stakeholders' summary report (2022). *International Journal of Enhanced Research in Educational Development*, *13*(2), 185–219.

[2] Bouattoura, F. (2025b). A fibristic epistemology for AI tool evaluation: A logic-based simulation framework. *International Journal of Enhanced Research in Educational Development*, *13*(3), 125–144.

[3] Bouattoura, F. (2025c). Significance in the Farid–El Djezairi triangular structure: Statistical and geometric analysis of positional ratios. *International Journal of Enhanced Research in Educational Development*, *13*(3), 100–124.

[4] Bouattoura, F. (2024). *Overcoming barriers with AI: Developing the El Djezairi tool to expose international structural inequalities through UPR analysis* [Unpublished doctoral proposal]. St. John's University.

Appendix A: *Structured Numeric Interval Ratios and Systematic Relationships*

Statement Number	Level 1	Level 2	Nested
1	1	0	0
2	0.375	0.5	0.625
3	0.181818	0.545455	0.636364
4	0.333333	0.666667	0.666667
5	0.666667	0.333333	0.333333
6	1	0	0
7	0.444444	0.555556	0.555556
8	0.428571	0.428571	0.571429
9	0.666667	0.333333	0.333333
10	0.3	0.7	0.7
11	1	0	0
12	1	0	0
13	0.6	0.4	0.4
14	0.5	0.5	0.5
15	0.666667	0.333333	0.333333
16	1	0	0
17	0.333333	0.416667	0.666667
18	0.5	0.5	0.5
19	1	0	0
20	1	0	0
21	1	0	0
22	0.666667	0.333333	0.333333
23	0.4	0.4	0.6
24	0.5	0.5	0.5
25	0.5	0.5	0.5
26	0.571429	0.428571	0.428571
27	0.625	0.375	0.375
28	0.333333	0.666667	0.666667
29	0.666667	0.333333	0.333333
30	0.833333	0.166667	0.166667
31	0.5	0.25	0.5
32	0.333333	0.333333	0.666667
33	1	0	0
34	0.375	0.375	0.625
35	0.6	0.2	0.4
36	1	0	0
37	1	0	0
38	0.5	0.5	0.5
39	0.666667	0.333333	0.333333
40	0.5	0.375	0.5
41	0.666667	0.333333	0.333333
42	1	0	0
43	0.428571	0.428571	0.571429
44	0.571429	0.285714	0.428571
45	0.6	0.2	0.4
46	0.5	0.25	0.5
47	0.5	0.5	0.5
48	0.75	0.25	0.25
49	0.6	0.2	0.4
50	0.571429	0.285714	0.428571
51	0.666667	0.166667	0.333333
52	0.666667	0.333333	0.333333
53	0.571429	0.428571	0.428571
54	0.5	0.333333	0.5
55	1	0	0
56	0.428571	0.428571	0.571429
57	0.75	0.25	0.25
58	0.5	0.375	0.5
59	0.375	0.5	0.625
60	0.666667	0.333333	0.333333
61	0.666667	0.333333	0.333333
62	0.8	0.2	0.2
63	0.5	0.375	0.5
64	0.6	0.2	0.4

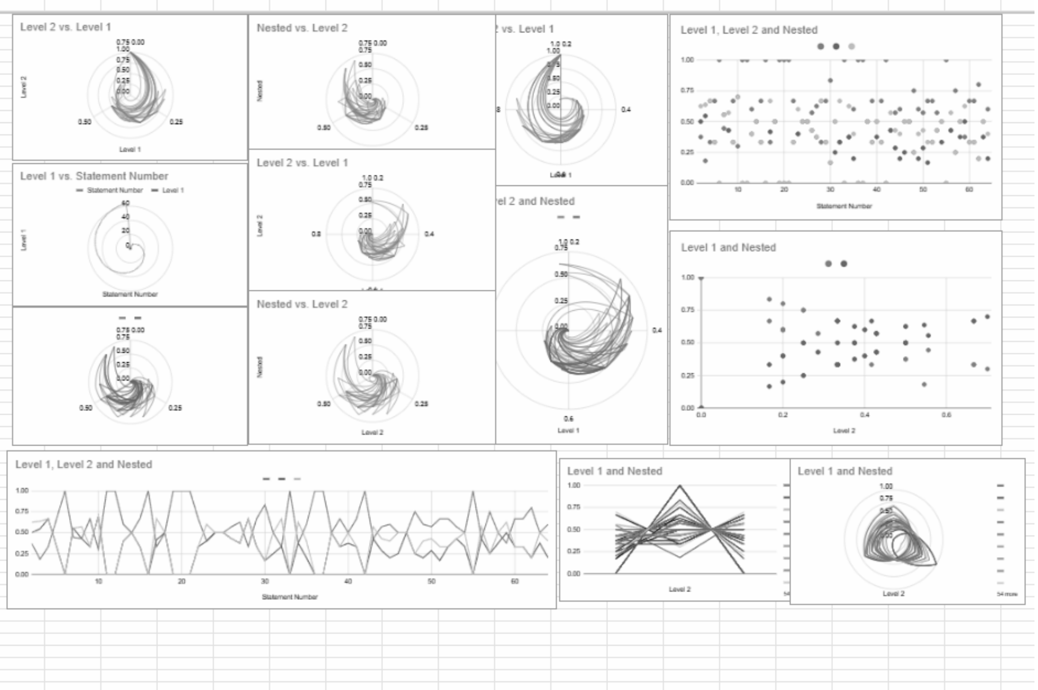

International Journal of Enhanced Research in Management & Computer Applications,
ISSN: 2319-7471, Volume 14 Issue 7, July 2025

Appendix B: Farid–El Djezairi Triangular Structure Numeric Ratios and Visualizations

	A	B	C	D	E	F	G	H	I	J	K	L	M	N	O	P
1		0	1	2	3	4	5	6	7	8	9	10	11	12	13	14
2	0								0							
3	1							0	1							
4	2							0	0.5	1						
5	3						0	0.3333	0.6667	1						
6	4						0	0.25	0.5	0.75	1					
7	5					0	0.2	0.4	0.6	0.8	1					
8	6					0	0.1667	0.3333	0.5	0.6667	0.8333	1				
9	7				0	0.1429	0.2857	0.4286	0.5714	0.7143	0.8571	1				
10	8				0	0.125	0.25	0.375	0.5	0.625	0.75	0.875	1			
11	9			0	0.1111	0.2222	0.3333	0.4444	0.5556	0.6667	0.7778	0.8889	1			
12	10			0	0.1	0.2	0.3	0.4	0.5	0.6	0.7	0.8	0.9	1		
13	11		0	0.0909	0.1818	0.2727	0.3636	0.4545	0.5455	0.6364	0.7273	0.8182	0.9091	1		
14	12		0	0.0833	0.1667	0.25	0.3333	0.4167	0.5	0.5833	0.6667	0.75	0.8333	0.9167	1	
15	13	0	0.0769	0.1538	0.2308	0.3077	0.3846	0.4615	0.5385	0.6154	0.6923	0.7692	0.8462	0.9231	1	
16	14	0	0.0714	0.1429	0.2143	0.2857	0.3571	0.4286	0.5	0.5714	0.6429	0.7143	0.7857	0.8571	0.9286	1
17		0	1	2	3	4	5	6	7	8	9	10	11	12	13	14

Appendix C: Planar Numeric Ratio Visualization and Positional Mapping

1	Level1 R	Level 2R	NestedR	Level1C	Level 2C	NestedC
2	8	2	8	6	7	8
3	11	11	8	3	7	11
4	3	7	3	6	3	7
5	3	6	3	7	3	6
6	1	6	1	7	1	6
7	9	9	7	6	7	9
8	6	7	7	7	6	7
9	3	6	3	7	3	6
10	10	10	9	5	9	10
11	1	6	1	7	1	6
12	1	6	1	7	1	6
13	5	5	6	7	6	5
14	7	2	7	2	7	2
15	3	6	3	7	3	
16	1	6	1	7	1	
17	3	6	3	6	12	
18	7	2	7	2	7	
19	1	6	1	7	1	
20	1	6	1	7	1	
21	1	6	1	7	1	
22	3	6	3	7	3	
23	6	5	5	5	6	
24	7	2	7	2	7	
25	7	2	7	2	7	
26	7	7	6	7	6	
27	8	6	8	8	8	
28	3	7	3	6	3	
29	3	6	3	7	3	
30	6	6	5	9	5	
31	7	4	7	2	6	
32	3	6	3	6	3	7
33	1	6	1	7	1	6
34	8	6	8	6	8	8
35	5	5	6	7	5	5
36	1	6	1	7	1	6
37	1	6	1	7	1	6
38	7	2	7	2	7	2
39	3	6	3	7	3	6
40	7	6	7	2	8	2
41	3	6	3	7	3	6
42	1	6	1	7	1	6
43	6	7	7	7	6	7
44	7	7	6	7	5	7
45	5	5	6	7	5	5
46	7	4	7	2	6	2
47	7	2	7	2	7	2
48	4	4	6	9	6	4
49	5	5	6	7	5	5
50	7	7	6	7	5	7
51	3	6	3	7	5	6
52	3	6	3	7	3	6
53	7	7	6	7	6	7
54	7	6	7	2	3	2
55	1	6	1	7	1	6
56	6	7	7	7	6	7
57	4	4	6	9	6	4
58	7	6	7	2	8	2
59	8	2	8	6	7	8
60	3	6	3	7	3	6
61	3	6	3	7	3	6
62	5	5	5	8	5	5
63	7	6	7	2	8	2
64	5	5	6	7	5	5